

Cite this: DOI: 10.1039/c8ta11172c

Received 21st November 2018
Accepted 22nd December 2018

DOI: 10.1039/c8ta11172c

rsc.li/materials-a

Photocatalytic dehydrogenation of formic acid promoted by a superior PdAg@g-C₃N₄ Mott–Schottky heterojunction†

Hu Liu,[‡] Xinyang Liu,^{‡,a} Weiwei Yang,^{*a} Mengqi Shen,^b Shuo Geng,^a Chao Yu,^b Bo Shen,^b and Yongsheng Yu,^{*a}

Herein, we report the production of a superior Mott–Schottky heterojunction that is based on PdAg nanowires (NWs) that grow *in situ* on graphitic carbon nitride (g-C₃N₄). Due to the strong Mott–Schottky effect between PdAg NWs and g-C₃N₄, the heterojunction enhances the photocatalytic dehydrogenation of formic acid (FA) (TOF = 420 h⁻¹) without additives and under visible light ($\lambda > 400$ nm) at 25 °C, which is the best value among all heterogeneous catalysts reported for the photocatalytic dehydrogenation of FA. The H₂ production rate is almost constant under the current reaction conditions. Detailed studies reveal that a favorable charge transfer from g-C₃N₄ and Ag to Pd makes Pd electron-rich, which enhances the catalytic activity and stability of the heterojunction for the photocatalytic dehydrogenation of FA under visible light. Our studies open up a new route to the design of a metal–semiconductor heterojunction for visible light-driven photocatalytic dehydrogenation of FA.

Exploitation of the secure and efficient dehydrogenation technology of hydrogen storage materials is an impending challenge as the entire world looks forward to replacing non-renewable fossil fuels in the future energy areas.¹ Among the hydrogen storage materials, formic acid (FA, HCOOH), a non-toxic renewable product, formed in biomass processing or the hydrogenation of carbon dioxide from industry with high energy density and liquid state at room temperature, has been considered as a promising energy carrier for a fuel-cell-based H₂ economy in the future.^{2–4} FA can be catalytically decomposed *via* a dehydrogenation (HCOOH \leftrightarrow H₂ + CO₂) or dehydration (HCOOH \leftrightarrow H₂O + CO) pathway. However, the undesirable dehydration pathway must be avoided because it produces CO,

which is a toxicant to fuel cell catalysts.^{4–6} Recently, significant efforts have been devoted towards the development of selective heterogeneous catalysts for the dehydrogenation route without the release of CO.^{7–10} Among the heterogeneous catalysts, Pd-based nanocatalysts show promising hydrogen generation rates for the FA decomposition under mild conditions. However, the poor H₂ selectivity and intrinsically weak CO tolerance of Pd can lead to reduced stability of the Pd-based nanocatalysts. Hence, tremendous efforts, including Pd-based nanoparticles (NPs),¹¹ nanowires (NWs),¹² nanosheets (NSs)¹³ and hollow nanospheres (NHSSs)¹⁴ structures, have been devoted to solving these issues.

In addition, the photocatalytic dehydrogenation of FA has attracted extensive interest as an efficient dehydrogenation technology to produce H₂ from FA under visible light at room temperature. Some reports show that the semiconductive supports that absorb visible light can be exploited to improve the photocatalytic performance of heterogeneous metal-catalysts for the photocatalytic dehydrogenation of FA;^{5–17} this is due to the electronic interaction and electron transfer between the metal and semiconductor, called Mott–Schottky effect, on the surface of metal–semiconductor interfaces.¹⁸ Therefore, the Mott–Schottky strategy was explored to enhance the photocatalytic dehydrogenation of FA with a coupled Pd-based catalyst with a semiconductive support through the strong metal–support interaction. Typical reported supports, including graphene oxide,¹⁹ metal–organic-framework (MOF),²⁰ SiO₂,²¹ TiO₂,²² and WO_{2.72},²³ are effective for the improvement of the photocatalytic dehydrogenation of FA due to their ability to tune the electronic/geometric structures of the nanocatalyst and the synergistic effect between the active Pd-based nanocatalyst and support. It is thus of great interest to have a semiconductor with a suitable majority-carrier type and band structure to build a Mott–Schottky heterojunction between the active nanocatalyst and support to adjust the surface charge density and catalytic property of the Pd-based nanocatalyst for the photocatalytic dehydrogenation of FA under visible light. Among the available semiconductors serving as a support, nanostructured graphitic

^aMIIT Key Laboratory of Critical Materials Technology for New Energy Conversion and Storage, School of Chemistry and Chemical Engineering, Harbin Institute of Technology, Harbin, Heilongjiang 150001, China. E-mail: yangww@hit.edu.cn

^bDepartment of Chemistry, Brown University, Providence, Rhode Island 02912, USA. E-mail: ysyu@hit.edu.cn

† Electronic supplementary information (ESI) available. See DOI: 10.1039/c8ta11172c

‡ These authors contribute equally.

carbon nitride ($g\text{-C}_3\text{N}_4$) with a band gap of 2.7 eV has been proven to be an ideal candidate²⁴ since the work function of some noble metals, such as Pd or Pt, are situated between the conduction and valence bands of $g\text{-C}_3\text{N}_4$.²⁵

In this study, we built the superior Mott–Schottky heterojunction based on PdAg NWs and $g\text{-C}_3\text{N}_4$ for the enhancement of the photocatalytic dehydrogenation of FA, as shown in Scheme 1. The photocatalytic heterojunction was constructed *in situ* by growing PdAg NWs on the surface of $g\text{-C}_3\text{N}_4$. Through a strong metal–support interaction between PdAg NWs and $g\text{-C}_3\text{N}_4$, the optimal Pd₅Ag₅ NWs@ $g\text{-C}_3\text{N}_4$ Mott–Schottky heterojunction exhibits an excellent catalytic performance for the photocatalytic dehydrogenation of FA (TOF = 420 h⁻¹) under additive-free conditions under visible light ($\lambda > 400$ nm) at 25 °C, which are the best values ever reported for a heterogeneous catalyst for the photocatalytic dehydrogenation of FA in an aqueous solution. The strategy demonstrates a new way to achieve low-cost visible light-driven dehydrogenation of FA.

The typical morphology and structure of the Pd₅Ag₅ NWs@ $g\text{-C}_3\text{N}_4$ Mott–Schottky heterojunction were characterized by transmission electron microscopy (TEM) with different magnifications and a representative high-resolution (HR) TEM images (Fig. 1A–C). It could be clearly observed that the *in situ* synthesized PdAg NWs, growing on the surface of $g\text{-C}_3\text{N}_4$, possess a network-like morphology with various convex/concave regions and kinks (Fig. 1A and B). The HR-TEM image shows the (111) lattice fringe distance of typical *in situ* synthesised face-centered cubic (fcc) PdAg alloy as 0.23 nm (Fig. 1C), which is between the (111) lattice spacing of fcc Ag (0.24 nm) and fcc Pd (0.22 nm). The Pd₅Ag₅ NWs@ $g\text{-C}_3\text{N}_4$ Mott–Schottky heterojunction was further characterized by HAADF-STEM image and scanning transmission electron microscopy-EDS (STEM-EDS) (Fig. 1D–G). Elemental mapping of the Pd₅Ag₅ NWs@ $g\text{-C}_3\text{N}_4$ Mott–Schottky heterojunction suggests that Pd and Ag disperse uniformly at the atomic level, which confirms that the homogeneous alloyed PdAg NWs have been successfully grown on the surface of $g\text{-C}_3\text{N}_4$. The PdAg NWs@ $g\text{-C}_3\text{N}_4$ Mott–Schottky heterojunction of different Ag and Pd compositions (Fig. S1†) was also synthesized by varying the molar ratio of the precursors. Their

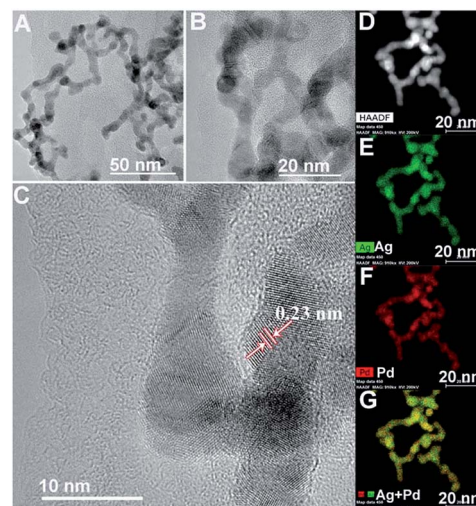
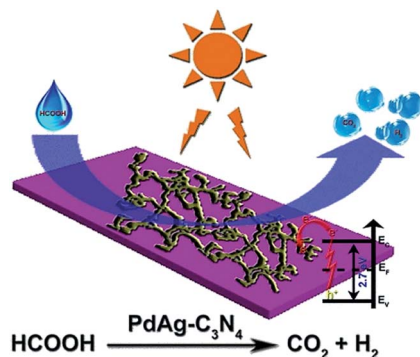


Fig. 1 (A and B) Typical TEM images of the Pd₅Ag₅ NWs@ $g\text{-C}_3\text{N}_4$ Mott–Schottky heterojunction at different magnifications. (C) HR-TEM image of the Pd₅Ag₅ NWs@ $g\text{-C}_3\text{N}_4$ Mott–Schottky heterojunction. (D–G) HAADF-STEM and elemental mapping of the Pd₅Ag₅ NWs@ $g\text{-C}_3\text{N}_4$ Mott–Schottky heterojunction.

compositions were analyzed by inductively coupled plasma optical emission spectroscopy (ICP-OES) (Table S1†). Fig. S2† shows the X-ray diffraction (XRD) patterns of the PdAg NWs@ $g\text{-C}_3\text{N}_4$ and Pd NWs@ $g\text{-C}_3\text{N}_4$ Mott–Schottky heterojunction. For the PdAg NWs@ $g\text{-C}_3\text{N}_4$ Mott–Schottky heterojunction, the XRD pattern exhibits the (111) plane of the fcc PdAg at 40°, and it has a weak peak of $g\text{-C}_3\text{N}_4$ at 27.5° attributed to the (002) plane of the $g\text{-C}_3\text{N}_4$ (JCPDS 87-1526),²⁶ further indicating that the PdAg NWs with an alloy structure have been *in situ* grown on the surface of $g\text{-C}_3\text{N}_4$.

To further investigate the effect of $g\text{-C}_3\text{N}_4$ on the electronic structures of Ag and Pd in the Pd₅Ag₅ NWs@ $g\text{-C}_3\text{N}_4$ Mott–Schottky heterojunction, we carried out the XPS measurement (Fig. S3† and 2A–D). As a control, the electronic states of C and N in $g\text{-C}_3\text{N}_4$ were also measured. It can be seen that



Scheme 1 Schematic of the enhanced activity of the PdAg@ $g\text{-C}_3\text{N}_4$ Mott–Schottky heterojunction for photocatalytic dehydrogenation of FA under visible light and schematic of a Mott–Schottky-type Pd₅Ag₅ NWs@ $g\text{-C}_3\text{N}_4$ contact (E_F : work function; E_C : conduction band; E_V : valence band).

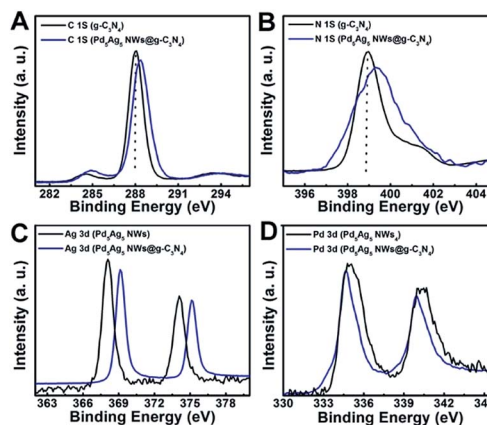


Fig. 2 (A and B) High resolution XPS spectra of C1s and N1s for $g\text{-C}_3\text{N}_4$ and Pd₅Ag₅ NWs@ $g\text{-C}_3\text{N}_4$ Mott–Schottky heterojunction, respectively. (C and D) High resolution XPS spectra of Ag 3d and Pd 3d for Pd₅Ag₅ NWs@ $g\text{-C}_3\text{N}_4$ Mott–Schottky heterojunction, respectively.

compared with those of pure $g\text{-C}_3\text{N}_4$, the binding energies of C1s and N1s from the Pd_5Ag_5 NWs@ $g\text{-C}_3\text{N}_4$ shifted to higher values (Fig. 2A and B). For the XPS spectra of Ag 3d and Pd 3d, the binding energies of Ag 3d_{3/2} in Pd_5Ag_5 NWs@ $g\text{-C}_3\text{N}_4$ Mott-Schottky heterojunction were also tested and found to be higher than those of Ag 3d_{3/2} in Pd_5Ag_5 NWs (Fig. 2C), whereas the binding energies for Pd 3d_{3/2} in Pd_5Ag_5 NWs@ $g\text{-C}_3\text{N}_4$ Mott-Schottky heterojunction shifted to lower values relative to those of the Pd_5Ag_5 NWs (Fig. 2D). These shifts demonstrate that electrons transfer from $g\text{-C}_3\text{N}_4$ and Ag to Pd in the Pd_5Ag_5 NWs@ $g\text{-C}_3\text{N}_4$ Mott-Schottky heterojunction. The shifts suggest that the Pd atoms are more electron-rich in the Pd_5Ag_5 NWs@ $g\text{-C}_3\text{N}_4$ Mott-Schottky heterojunction because $g\text{-C}_3\text{N}_4$ donates more electrons to Pd_5Ag_5 NWs and produces more electron-rich Pd centers with lower binding energies.²⁷ Therefore, the XPS spectra measurement verifies that the strong Mott-Schottky effect between $g\text{-C}_3\text{N}_4$ and Pd_5Ag_5 NWs increases the electron density of the Pd atoms and makes the Pd atoms more electron-rich in the Pd_5Ag_5 NWs@ $g\text{-C}_3\text{N}_4$ Mott-Schottky heterojunction because of the strong metal-support interaction. Overall, $g\text{-C}_3\text{N}_4$ towards Pd_5Ag_5 NWs increases the electron density of the Pd active centers; this facilitates the O-H cleavage and strengthens the adsorption of formate. $g\text{-C}_3\text{N}_4$ acts as a proton scavenger for the O-H bond dissociation to form the protonated $g\text{-C}_3\text{N}_4$, which further promotes the β -hydride elimination of Pd-formate intermediates to produce H_2 and CO_2 .²⁸

To choose an effective Mott-Schottky heterojunction, the catalytic activities of the PdAg NWs@ $g\text{-C}_3\text{N}_4$ Mott-Schottky heterojunction with different Ag or Pd composition were initially studied by plotting the volume of gas ($\text{CO}_2 + \text{H}_2$) versus the reaction time in a 10 mL FA aqueous solution (1 M) under visible light ($\lambda > 400$ nm) at 25 °C (Fig. S4A†). The initial TOF of Pd₇Ag₃ NWs@ $g\text{-C}_3\text{N}_4$, Pd₅Ag₅ NWs@ $g\text{-C}_3\text{N}_4$, Pd₃Ag₇ NWs@ $g\text{-C}_3\text{N}_4$ and Pd NWs@ $g\text{-C}_3\text{N}_4$ is 346, 420, 242, and 105 h⁻¹, respectively (Fig. S4B†). Pd₅Ag₅ NWs@ $g\text{-C}_3\text{N}_4$ has the highest catalytic activity among the PdAg NWs@ $g\text{-C}_3\text{N}_4$ with different Ag or Pd compositions. The evaluation shows that $g\text{-C}_3\text{N}_4$ can be used as an effective support to improve the PdAg NWs for use during the photocatalytic dehydrogenation of FA. As a control, we also chose a physical mixing method to prepare the catalyst by blending Pd₅Ag₅ NWs and $g\text{-C}_3\text{N}_4$ and then tested the catalytic activity of the mixture for H_2 generation from FA decomposition under visible light ($\lambda > 400$ nm) at 25 °C. It was found that the mixture exhibited a much poorer catalytic activity than the Pd₅Ag₅ NWs@ $g\text{-C}_3\text{N}_4$ Mott-Schottky heterojunction; this indicated that the Pd₅Ag₅ NWs@ $g\text{-C}_3\text{N}_4$ Mott-Schottky heterojunction had a stronger coupling between Pd₅Ag₅ NWs and $g\text{-C}_3\text{N}_4$ (Fig. 3A). In addition, the catalytic activities of Pd₅Ag₅ NWs without a support for H_2 generation from FA decomposition under visible light ($\lambda > 400$ nm) at 25 °C were measured (Fig. 3A). Obviously, the Pd₅Ag₅ NWs@ $g\text{-C}_3\text{N}_4$ Mott-Schottky heterojunction exhibits a much better catalytic activity than Pd₅Ag₅ NWs; this also suggests that the strong coupling effect between the Pd₅Ag₅ NWs and $g\text{-C}_3\text{N}_4$ is a key factor for improving the catalytic activity. In addition, the volume of the gas mixture generated versus time for Pd₅Ag₅ NWs@ $g\text{-C}_3\text{N}_4$ is linear, thus indicating that H_2 production rate is almost constant under the

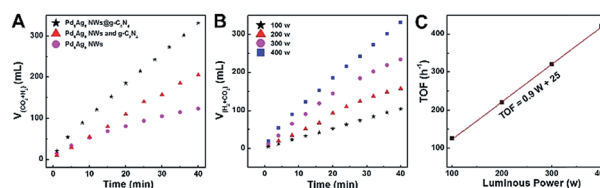


Fig. 3 (A) The volume of gas mixture ($\text{CO}_2 + \text{H}_2$) generated vs. time for the FA dehydrogenation catalysed by different catalysts in FA aqueous solution (10 mL of 1 M) under visible light irradiation ($\lambda > 400$ nm) at 25 °C, respectively. (B) The volume of gas mixture ($\text{CO}_2 + \text{H}_2$) generated vs. time for the photocatalytic dehydrogenation of FA and (C) TOF vs. power for Pd₅Ag₅ NWs@ $g\text{-C}_3\text{N}_4$ Mott-Schottky heterojunction at different light intensity in FA aqueous solution (10 mL, 1 M) under visible light irradiation ($\lambda > 400$ nm) at 25 °C.

current reaction condition; this is very important for practical H_2 application (Fig. 3A).

Since the dehydrogenation of FA is generally accompanied by the undesired FA dehydration reaction, we also measured the evolving gas mixture by gas chromatograph (GC), and there was no CO detected in the gas mixture (detection limit > 2 ppm) (Fig. S5 and S6†). Additionally, we measured the H_2 volumes by gas mixture flowing through the typical NaOH trap and then compared them with the gas mixture ($\text{CO}_2 + \text{H}_2$) volumes (Fig. S7†). These results demonstrate that the gas mixture is indeed composed of H_2 and CO_2 , and the molar ratio of CO_2 and H_2 is 1. Importantly, these results testify that CO-free H_2 can be released from our Mott-Schottky heterojunction.

We further studied the effects of catalyst concentration, FA concentration and temperature on the photocatalytic dehydrogenation of FA over the Pd₅Ag₅ NWs@ $g\text{-C}_3\text{N}_4$ Mott-Schottky heterojunction. At first, the dehydrogenation reaction was performed at different catalyst concentrations from 1.25 mM to 10 mM by keeping the FA concentration at 1.0 M and visible light irradiation ($\lambda > 400$ nm) at 25 °C. The volume of the generated gas versus the reaction time during the photocatalytic dehydrogenation of FA at different catalyst concentrations is plotted in Fig. S8A.† The rate of FA dehydrogenation reaction of the corresponding catalyst concentration was calculated by the volume of the generated gas during the initial 10 minutes. The slope of the line plotted the logarithmic value of the hydrogen generation rate versus the catalyst concentration is 1.01 (Fig. S8B†), demonstrating that the photocatalytic dehydrogenation of FA follows pseudo-first-order kinetic at different catalyst concentrations.

We also studied the effect of visible light intensity on the photocatalytic dehydrogenation of FA over the Pd₅Ag₅ NWs@ $g\text{-C}_3\text{N}_4$ Mott-Schottky heterojunction at a 10 mM concentration and 1 M aqueous FA solution under visible light irradiation ($\lambda > 400$ nm) (Fig. 3B). It was found that the rate of FA dehydrogenation increased linearly with the increasing light intensities (TOF = 0.9 W + 25) (Fig. 3C); this indicated that the catalytic activity of our Mott-Schottky heterojunction was easily controlled by the light intensity. It also demonstrates the great promise of the PdAg NWs@ $g\text{-C}_3\text{N}_4$ Mott-Schottky heterojunction as a more practical photocatalyst for FA dehydrogenation. In addition, to study the effect of the FA concentration

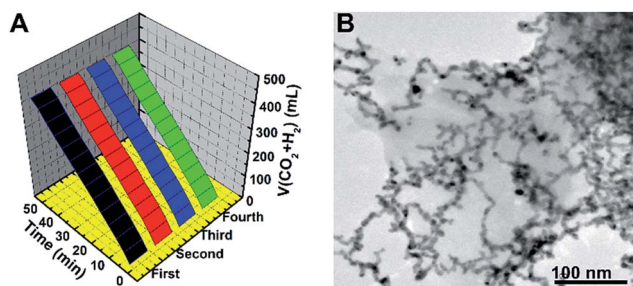


Fig. 4 (A) The stability of Pd₅Ag₅ NWs@g-C₃N₄ Mott-Schottky heterojunction in aqueous FA solution (10 mL, 1 M) under visible light ($\lambda > 400$ nm) at 25 °C. (B) TEM image of the Pd₅Ag₅ NWs@g-C₃N₄ Mott-Schottky heterojunction after the four catalytic runs.

on the gas-generation rate, the concentration of the Pd₅Ag₅ NWs@g-C₃N₄ Mott-Schottky heterojunction was kept constant at 10 mM under visible light ($\lambda > 400$ nm) at 25 °C. The volume of gas-generation *versus* reaction time is plotted at different FA concentrations (Fig. S9A†). Fig. S9B† shows the initial TOFs *versus* corresponding FA concentration plot. When the FA concentration was increased from 0.125 M to 1.0 M, the gas-generation rate increased linearly ($\text{TOF} = -771.6C_{\text{FA}} - 167.5$), but dropped when the FA concentration was higher than 1 M; this result verified that the gas-generation rate was closely related to the FA concentration.

Finally, the catalytic stability of the Pd₅Ag₅ NWs@g-C₃N₄ Mott-Schottky heterojunction was tested in an aqueous FA solution (10.0 mL, 1.0 M) under visible light ($\lambda > 400$ nm, 400 W) at 25 °C. The Pd₅Ag₅ NWs@g-C₃N₄ Mott-Schottky heterojunction maintained its initial activity in the aqueous FA solution after the catalyst was used for four cycles (Fig. 4A). We further investigated the morphology (Fig. 4B) and composition (Tables S3 and S4†) of the Pd₅Ag₅ NWs@g-C₃N₄ catalyst after the fourth run using XPS, ICP-AES and TEM. There was no obvious change in the C/N and Ag/Pd composition, the Pd₅Ag₅ NWs with a network-like morphology were still anchored on the surface of the g-C₃N₄, and there was no Ag and Pd in our catalytic system of the liquid phase. This result indicates that the Pd₅Ag₅ NWs@g-C₃N₄ Mott-Schottky heterojunction is sufficiently stable and recyclable for the photocatalytic dehydrogenation of FA under visible light ($\lambda > 400$ nm) at 25 °C.

Conclusions

In summary, we presented an ingenious strategy to optimize the catalytic activity of PdAg NWs toward the dehydrogenation of FA by *in situ* growth of PdAg NWs on the surface of semiconductive g-C₃N₄ to build a Mott-Schottky heterojunction. Due to the Mott-Schottky effect between g-C₃N₄ and the PdAg NWs, the Pd₅Ag₅ NWs@g-C₃N₄ Mott-Schottky heterojunction has the highest activity with an initial TOF of up to 420 h⁻¹ under additive-free conditions under visible light ($\lambda > 400$ nm) at 25 °C. Detailed studies on the Pd₅Ag₅ NWs@g-C₃N₄ Mott-Schottky heterojunction reveal that a favorable charge transfer from g-C₃N₄ and Ag to Pd makes Pd electron-rich, which leads to the

enhancement of the catalytic activity of the Pd₅Ag₅ NWs@g-C₃N₄ Mott-Schottky heterojunction, which has a boosting activity and superior stability for the photocatalytic dehydrogenation of FA under visible light. This study opens a new method to design high-performance heterogeneous catalysts with a Mott-Schottky effect by visible light as a driving force to trigger the FA dehydrogenation to meet practical H₂-based energy device applications.

Conflicts of interest

There are no conflicts of interest to declare.

Acknowledgements

This work was supported by the National Natural Science Foundation of China under Grant (No. 51571072 and 51871078), Fundamental Research Funds for the Central Universities (No. AUGA5710012715), Heilongjiang Science Foundation (No. E2018028), China Postdoctoral Science Foundation (No. 2015M81436), Heilongjiang Postdoctoral Science Foundation (No. LBH-Z15065) and China Scholarship Council.

Notes and references

- 1 L. Schlapbach and A. Züttel, *Nature*, 2001, **414**, 353–358.
- 2 B. Loges, A. Boddien, F. Gärtner, H. Junge and M. Beller, *Top. Catal.*, 2010, **53**, 902–914.
- 3 M. Grasmann and G. Laurenczy, *Energy Environ. Sci.*, 2012, **5**, 8171–8181.
- 4 T. C. Johnson, D. J. Morris and M. Wills, *Chem. Soc. Rev.*, 2010, **39**, 81–88.
- 5 P. J. Hausoul, C. Broicher, R. Vegliante, C. Göb and R. Palkovits, *Angew. Chem., Int. Ed.*, 2016, **55**, 5597–5601.
- 6 Z. L. Wang, J. M. Yan, Y. Ping, H. L. Wang, W. T. Zheng and Q. Jiang, *Angew. Chem., Int. Ed.*, 2013, **52**, 4406–4409.
- 7 W. Y. Yu, G. M. Mullen, D. W. Flaherty and C. B. Mullins, *J. Am. Chem. Soc.*, 2014, **136**, 11070–11078.
- 8 A. Boddien, D. Mellmann, F. Gärtner, R. Jackstell, H. Junge, P. J. Dyson, G. Laurenczy, R. Ludwig and M. Beller, *Science*, 2011, **333**, 1733–1736.
- 9 (a) S. M. Barrett, S. A. Slattery and A. J. M. Miller, *ACS Catal.*, 2015, **5**, 6320–6327; (b) H. Liu, Y. Y. Yu, W. W. Yang, W. J. Lei, M. Y. Gao and S. J. Guo, *Nanoscale*, 2017, **9**, 9305–9309.
- 10 Y. Chen, Q. L. Zhu, N. Tsumori and Q. Xu, *J. Am. Chem. Soc.*, 2015, **137**, 106–109.
- 11 (a) S. Zhang, O. Metin, D. Su and S. H. Sun, *Angew. Chem., Int. Ed.*, 2013, **52**, 3681–3684; (b) K. Tedsree, T. Li, S. Jones, C. W. A. Chan, K. M. K. Yu, P. A. J. Bagot, E. A. Marquis, G. D. W. Smith and S. C. E. Tsang, *Nat. Nanotechnol.*, 2011, **6**, 302.
- 12 (a) H. Liu, Y. Y. Yu, W. W. Yang, W. J. Lei, M. Y. Gao and S. J. Guo, *Nanoscale*, 2017, **9**, 9305–9309; (b) H. Liu, Y. Guo, Y. Y. Yu, W. W. Yang, M. Q. Shen, X. Y. Liu, S. Geng, J. R. Li, C. Yu, Z. Y. Yin and H. B. Li, *J. Mater. Chem. A*, 2018, **6**, 17323–17328; (c) H. Liu, X. Y. Liu, Y. Y. Yu,

- W. W. Yang, J. Li, M. Feng and H. B. Li, *J. Mater. Chem. A*, 2018, **6**, 4611–4616.
- 13 C. Y. Hu, X. L. Mu, J. M. Fan, H. B. Ma, X. J. Zhao, G. X. Chen, Z. Y. Zhou and N. F. Zheng, *Chem. Nanostruct. Mater.*, 2016, **2**, 28–32.
- 14 Y. Q. Jiang, X. L. Fan, X. Z. Xiao, T. Qin, L. T. Zhang, F. L. Jiang, M. Li, S. Q. Li, H. W. Ge and L. X. Chen, *J. Mater. Chem. A*, 2016, **4**, 657–666.
- 15 L. Xiao, Y. S. Jun, B. Wu, D. Liu, T. T. Chuong, J. Fan and S. G. D. Tucky, *J. Mater. Chem. A*, 2017, **5**, 6382–6387.
- 16 M. F. Kuehnel, D. W. Wakerley, K. L. Orchard and E. Reisner, *Angew. Chem., Int. Ed.*, 2015, **54**, 9627–9631.
- 17 Y. Y. Cai, X. H. Li, Y. N. Zhang, X. Wei, K. X. Wang and J. S. Chen, *Angew. Chem., Int. Ed.*, 2013, **52**, 11822–11825.
- 18 X. H. Li and M. Antonietti, *Chem. Soc. Rev.*, 2013, **42**, 6593–6604.
- 19 Y. Ping, J. M. Yan, Z. L. Wang, H. L. Wang and Q. Jiang, *J. Mater. Chem. A*, 2013, **1**, 12188–12191.
- 20 X. Gu, Z.-H. Lu, H.-L. Jiang, K. Akita and Q. Xu, *J. Am. Chem. Soc.*, 2011, **133**, 11822.
- 21 Q. G. Liu, X. F. Yang, Y. Q. Huang, S. T. Xu, X. Su, X. L. Pan, J. M. Xu, A. Q. Wang, C. H. Liang, X. K. Wang and T. Zhang, *Energy Environ. Sci.*, 2015, **8**, 3204–3207.
- 22 M. Hattori, H. Einaga, T. Daio and M. Tsuji, *J. Mater. Chem. A*, 2015, **3**, 4453–4461.
- 23 C. Yu, X. F. Guo, Z. Xi, M. Michelle, Z. Y. Yin, B. Shen, J. R. Li, C. Seto and S. H. Sun, *J. Am. Chem. Soc.*, 2017, **139**, 5712–5715.
- 24 (a) J. Y. Li, W. Cui, Y. J. Sun, Y. H. Chu, W. L. Cen and F. Dong, *J. Mater. Chem. A*, 2017, **5**, 9358–9364; (b) W. Cui, J. J. Li, F. Dong, Y. J. Sun, G. G. Jiang, W. L. Cen, S. C. Lee and Z. B. Wu, *Environ. Sci. Technol.*, 2017, **51**, 10682–10690; (c) W. Cui, J. J. Li, Y. J. Sun, H. Wang, G. M. Jiang, S. C. Lee and F. Dong, *Appl. Catal., B*, 2018, **237**, 938–946.
- 25 (a) Y. Y. Cai, X. H. Li, Y. N. Zhang, Z. Wei, K. X. Wang and J. S. Chen, *Angew. Chem., Int. Ed.*, 2013, **52**, 11822–11825; (b) W. Che, W. R. Cheng, T. Yao, F. M. Tang, W. Liu, H. Su, Y. Y. Huang, Q. H. Liu, J. K. Liu, F. C. Hu, Z. Y. Pan, Z. H. Sun and S. Q. Wei, *J. Am. Chem. Soc.*, 2017, **139**, 3021–3026.
- 26 H. J. Li, B. W. Sun, L. Sui, D. J. Qian and M. Chen, *Phys. Chem. Chem. Phys.*, 2015, **17**, 3309–3315.
- 27 H. Tsunoyama, N. Ichikuni, H. Sakurai and T. Tsukuda, *J. Am. Chem. Soc.*, 2009, **131**, 7086–7093.
- 28 H. Liu, B. L. Huang, J. H. Zhou, K. Wang, Y. S. Yu, W. W. Yang and S. J. Guo, *J. Mater. Chem. A*, 2018, **6**, 1979–1984.